JULY 12–16 2020 VIRTUAL JOINT AAPM | COMP MEETING
EASTERN TIME [GMT-4]

Control Point-Specific Repositioning to Reduce the Dosimetric Impact of Intrafraction Motion for Small Targets Treated with Virtual Cones

C Church[1], D Parsons[2], A Syme[1,3]
(1)Dalhousie University, Halifax, NS, CA
(2)UT Southwestern Medical Center, Dallas, TX
(3)Department of Radiation Oncology, Halifax, NS, CA

DALHOUSIE UNIVERSITY
nova scotia health authority

INTRODUCTION

Intrafraction patient motion is an unavoidable occurrence during any treatment that leads to dosing-errors for the planning target volume (PTV) and surrounding healthy tissue. Many centers will implement various measures to mitigate patient motion such as the use of a thermoplastic immobilization mask during stereotactic radiosurgery (SRS). However, even with the use of thermoplastic masks, patient motion does occur. [1,2] To treat small targets with SRS most centers rely on the use of stereotactic cones which can elongate the duration of therapy. It has been shown that an increase in treatment length correlates with larger positional shifts.[3]

To minimize the effects of intra-fraction motion we will make use of two techniques:

- Utilize apertures shapes by the multileaf collimator (MLC) to create virtual cones, reducing the time-sink needed for setting-up stereotactic cones. Virtual cones have been shown to have comparable dosimetry when compared with stereotactic cones.[4]
- Use periodic imaging with the 2.5 MV beam within a Truebeam linear accelerator (Varian Medical Systems, Palo Alto, CA) to detect and offset motion with respect to the beams-eye-view.

AIM

1. To investigate the dosimetric impacts of intra-fraction patient motion using a MAX-HD head phantom.
2. To investigate if control point-specific repositioning can be used to improve targeting accuracy and dosimetric conformity.
3. Explore the impacts of different aperture sizes on intra-fraction motion using a water phantom with Monte Carlo (MC) simulations.

METHODS

Monte Carlo:
A single MLC-defined beamlet was incident upon an 8.2 cm water sphere with a 0.25 mm isotropic voxel size using the EGSnrc MC tool to create a dose kernel as shown in Figure 1. Performing a superposition of the dose kernel in MATLAB, a dose-distribution was created for a treatment with a co-planar arc as well as two non-coplanar arcs with the couch at ± 45° as shown in Figure 2. This analysis was repeated for a variety of different aperture sizes.

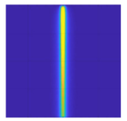

Figure 1. Dose-kernel for 2.1 x 5 mm² field

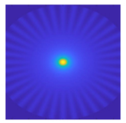

Figure 2. Axial slice of a delivery with a coplanar arc as well as two non-coplanar arcs.

Machine Delivery:
A single sheet of gafchromic film with a metal-bb attached was inserted as a sagittal slice inside of the MAX-HD phantom as shown in Figure 3.B.

Treatment consisted of two co-planar arcs with 2.1 x 5 mm² field shaped by the MLC. Two arcs were delivered with the collimator at ± 45° with 50 monitor units delivered every 10 degrees of gantry movement.

The phantom was moved linearly from its initial position until it was 1.44 mm offset along each axis by the end of treatment. To reposition the phantom at each control point two different methodologies were implemented:

BB-tracking: The metal-bb attached to the film acted as a surrogate for our treatment center as was done in our previously published work.[5] A diamond aperture was used to image the bb at each control point and its position relative to the aperture centre was used to calculate necessary couch shifts as shown in Figure 3.C.

Anatomy tracking: MV images were acquired at each control point with the EPID and were registered to MATLAB-generated DRRs with mutual information. The MLC was used to acquire images only containing bony anatomy as shown in Figure 3.D, and the registration results were used to re-align the phantom with couch shifts.[6] Each image was ensured to not contain the metal-bb within the frame.

Films were scanned at 400 dpi and converted to dose distributions using triple channel film dosimetry.[7]

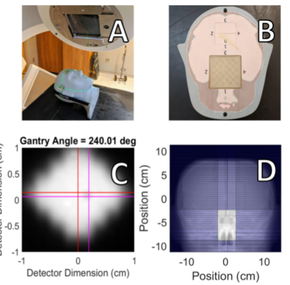

Figure 3. (A) MAX-HD phantom aligned to laser pre-treatment. (B) 3D-printed film holder inside of phantom. (C) Tracking metal-bb position glued to film. (D) Tracking anatomy using MLC-defined aperture.

RESULTS

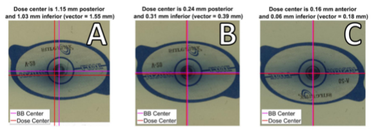

Figure 4. (A) Film irradiated with moving phantom. (B) Film irradiated with phantom repositioning using bb-tracking. (C) Film irradiated with phantom repositioning using anatomy tracking.

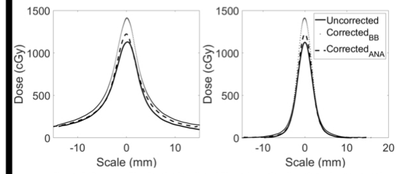

Figure 5. Dose profiles for the irradiated films along the direction of gantry motion (left) and perpendicular to gantry motion (right). *BB represents repositioning with bb-tracking and ANA represents repositioning with anatomy-tracking.*

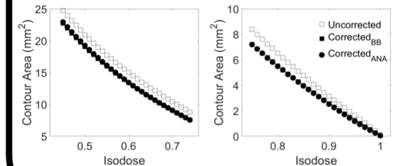

Figure 6. Isodose area from above films for 45 - 75% of the max dose (left) and 76 – 100% of the max dose (right).

The film scans used to determine targeting accuracy (defined as the 2D distance of the metal-bb to the dose centre) are as shown in Figure 4. When using anatomy tracking to reposition the phantom, targeting accuracy was found to be 0.18 mm compared to 1.55 mm when no re-positioning was implemented. When repositioning the phantom with bb-tracking, the targeting accuracy was found to be 0.39 mm.

Using these two repositioning methods, the maximum dose was found to being increased by 8.6% when using anatomy-tracking and 23.6% when using bb-tracking as shown in Figure 5.

Both tracking methods exhibited quantitatively similar improvements in dose compactness as shown in Figure 6 by reducing the dose area by ~19% at the 90% isodose, ~13% at the 70% isodose, and ~9% at the 50% isodose when compared to no phantom re-alignment. It is worth noting that each analysis had the dose-distribution normalized to its' own maximum dose.

Various metrics pulled from the dose volume histogram figures 7/8. *V_{Rx} is the target volume receiving the prescription dose of 100%. $D_{5\%}$ is the dose received by 5% of the volume for the respective volume indicated.*

Aperture size:	2.1 x 5 mm (4 mm target)		2.1 x 5 mm (2 mm target)		6 x 10 mm (8 mm target)		6 x 10 mm (4 mm target)	
Metric	Movement	Stationary	Movement	Stationary	Movement	Stationary	Movement	Stationary
V_{Rx} (%)	69	99	4	99	82	99	40	99
$D_{5\%}$, 1 mm shell	143	110	100	103	120	116	103	101
$D_{5\%}$, 2 mm shell	125	86	96	89	110	108	101	98
$D_{5\%}$, 3 mm shell	106	67	89	73	101	103	93	93

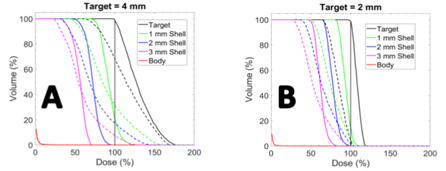

Figure 7. Dose volume histogram from MC simulations with 2.1 x 5 mm² field, solid lines represent delivery without movement, dashed lines represent a delivery with phantom movement. (A) is a dose volume histogram for a 4 mm spherical target and (B) is for a 2 mm spherical target.

Analyzing the dose volume histograms (DVH) for a few representative cases, we can evaluate the dosimetric trade-offs when using different aperture sizes and the impact of intrafraction motion. When treating the same sized target with different field sizes (2.1 x 5 mm^5 vs. 6 x 10 mm^2) as shown in Figure 7.A and 8.B, we see that a smaller field size produces a sharper dose-gradient as the concentric shells surrounding the target receive less dose. However, when motion is present, the smaller field sizes produces larger hot spots in the surrounding tissue. When treating different target sizes with a larger aperture, we see that the relative penalties of motion (smaller V_{Rx}, and larger $D_{5\%}$ to surrounding tissue) become less severe at the expense of delivering a larger absolute dose to the tissues surrounding the target.

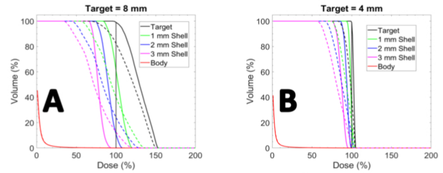

Figure 8. Dose volume histogram from MC simulations with 6 x 10 mm² field, solid lines represent delivery without movement, dashed lines represent a delivery with phantom movement. (A) is a dose volume histogram for a 8 mm spherical target and (B) is for a 4 mm spherical target.

CONCLUSIONS

This work demonstrates the impacts of intrafraction motion on dosimetric outcomes when treating small targets:

- **Smaller field sizes have the benefit of maximizing dose compactness.**
  - **Risk of larger dose-penalties to surrounding tissues when motion is present.**
- **Impact of intrafraction motion can be mitigated by implementing control point-specific image registration.**

In the future we plan to implement non-coplanar deliveries with simulated patient motion.

CONTACT INFORMATION

Cody Church / Email: cody.church@dal.ca
Alasdair Syme / Alasdair.Syme@nshealth.ca

REFERENCES

1. Kataria T et al. Analysis of intrafraction motion in CyberKnife-based stereotaxy using mask based immobilization and 6D-skull tracking. *Jour of Radiosurgery and SBRT 2016; 4; 2013 - 12.*
2. MacDonald R.L. et al. Real-time infrared motion tracking analysis for patients treated with gated frameless image guided stereotactic radiosurgery. *Int J Radiation Oncol Biol Phys 2020; 106(2); 413 – 21.*
3. Lewis B.C. Monitoring frequency of intra-fraction patient motion using the ExacTrac system for LINAC-based SRS treatments. *J Appl Clin Med Phys 2018; 19(3); 58 – 63.*
4. Popple R.A. The virtual cone: A novel technique to generate spherical dose distributions using a multileaf collimator and standardized control-point sequence for small target radiation surgery. *Adv Radiat Oncol 2018 3; 421 – 30.*
5. Parsons D et al. Toward a pre-clinical irradiator using clinical infrastructure. *Physica Medica 2019; 58; 21 – 31.*
6. Church C et al. Sub-mm Positioning Accuracy Using MV Arc-based Imaging for Virtual Isocenter Treatments. *COMP abstract 2019.*
7. Mayer RR et al. Enhanced Dosimetry Procedures and Assessment for EBT2 Radiochromic Film. *Med Phys 2012; 39(4); 2147 – 55.*